The Biomaterial-Induced Cellular Reaction Allows a Novel Classification System Regardless of the Biomaterials Origin

Sarah Al-Maawi, DMD[1]
James L. Rutkowski, DMD, PhD[2]
Robert Sader, MD, DMD, PhD[1]
C. James Kirkpatrick, MD, PhD[1]
Shahram Ghanaati, MD, DMD, PhD[1]*

Several different biomaterials are being introduced for clinical applications. However, no current material-specific systematic studies define parameters for evaluating these materials. The aim of this retrospective animal study is to classify biomaterials according to the in vivo induced cellular reaction and outline the clinical consequence of the biomaterial-specific cellular reaction for the regeneration process. A retrospective histologic analysis was performed for 13 polymeric biomaterials and 19 bone substitute materials (BSMs) (of various compositions and origins) that were previously implanted in a standardized subcutaneous model. Semiquantitative analyses were performed at days 3, 15, and 30 after implantation according to a standardized score for the induction of multinucleated giant cells (MNGCs) and vascularization rate. The induced cellular reaction in response to different polymeric materials allowed their classification according to the MNGC score in the following groups: class I induced no MNGCs at any time point, class II induced and maintained a constant number of MNGCs over 30 days, and class III induced MNGCs and provided an increasing number over 30 days. All BSMs induced MNGCs to varying extents. Therefore, the resultant BSM classifications are as follows: class I induced MNGCs with a decreasing number, class II induced and maintained constant MNGCs over 30 days, and class III induced MNGCs with increasing number over 30 days. These observations were mostly related to the biomaterial physicochemical properties and were independent of the biomaterial origin. Consequently, the induction of MNGCs and their increase over 30 days resulted in disintegration of the biomaterial. By contrast, the absence of MNGCs resulted in an integration of the biomaterial within the host tissue. This novel classification provides clinicians a tool to assess the capacity and suitability of biomaterials in the intended clinical indication for bone and soft tissue implantations.

Key Words: biomaterials, multinucleated giant cells, MNGCs, cellular reaction, inflammatory pattern

INTRODUCTION

Modern dentistry aims to restore the physiologic form, function, and esthetics of a single lost tooth or multiple teeth. Therefore, oral and maxillofacial surgery focuses on the placement of dental implants to optimize tooth restoration and improve the patient's quality of life.[1] However, for successful implant fixation and osseointegration, a defined bone volume is required.[2] In addition to autologous bone transplantation, different biomaterials have been introduced to provide a minimally invasive method for supporting guided bone regeneration (GBR). For long-term success, sufficient peri-implant soft tissue is essential to prevent bacterial access to the implants.[3] Therefore, biomaterials should also be able to support soft tissue regeneration in terms of guided tissue regeneration (GTR).

Among others, 2 groups of materials are the most important in clinical application in terms of GTR and GBR. These materials groups are polymeric membranes/matrices and bone substitute materials (BSMs). Membranes and matrices are applied either in combination with BSMs or alone depending on the clinical situation.[4]

Numerous types of biomaterials for medical use are currently available in the marketplace.[5] To study these materials systematically, a classification method would be helpful. The classification method would need to consider the materials composition, properties, and most importantly their role in the regeneration process.

In general, biomaterials are classified according to their ability to resorb (ie, resorbable or nonresorbable materials).[6] This specific property is essential to define the advantages and disadvantages of biomaterials and thereby assess their suitability in various clinical situations.[7] Biomaterials can also be classified according to their origin (ie, synthetically manufactured or naturally derived).[8] Different chemical compositions are used to produce polymeric biomaterials and BSMs. In the case of resorbable BSMs, hydroxyapatite, tricalcium phosphate, and their combinations are widely used.[9] Resorbable synthetic polymers, such as polycaprolacton (PCL),[10] polylactic acid (PLA),[11] and poly(lactic-co-glycolic acid) (PLGA)[12] have demonstrated successful and promising results as BSMs and polymeric membranes in varied surgical fields. Among the

[1] FORM-Lab, Frankfurt Oral Regenerative Medicine, Department for Oral, Cranio-Maxillofacial and Facial Plastic Surgery, Medical Center of the Goethe University, Frankfurt, Germany.
[2] Restorative Dentistry, School of Dental Medicine, State University of New York, Buffalo, NY.
* *Corresponding author, e*-mail: shahram.ghanaati@kgu.de
https://doi.org/10.1563/aaid-joi-D-19-00201

group of nonresorbable synthetic materials, especially in the field of periodontology, polytetrafluorethylene (PTFE) membranes have demonstrated good biocompatibility and provide a physical barrier when applied in terms of GBR and GTR.[13]

Naturally derived biomaterials are the most favorable in clinical applications.[14] Because of their natural structure and similarities to the human tissue structure, these materials are assumed to be most suitable for clinical use. Naturally derived materials are mostly classified according to their origin as allogeneic (human),[15] xenogeneic (animal),[16,17] or phycogeneic (plant).[18] In the group of BSMs, natural bone is obtained from the same or a different species and purified/processed to be suitable for human clinical applications. In this context, many manufacturers promise to preserve the natural architecture of the natural bone to gain the best clinical results.[19] In the group of polymeric biomaterials, collagen is the most favorable and widely used natural material.[20] Collagen is a highly preserved protein throughout species. Its ubiquitous occurrence in the extracellular matrix supports regeneration by offering an appropriate adherent surface for cells that are involved in the regeneration process.[21] Another natural polymeric biomaterial is silk fibroin, which is extracted from silk worms or spiders.[22] This resorbable biomaterial demonstrates a high degree of biocompatibility in vitro[23] and in vivo[10] and therefore is used as a suture material and a bone substitute material as well.[22,23]

Allogeneic and xenogeneic materials must undergo strict purification and processing procedures to eliminate pathogens and reduce the risk of immunogenicity.[19] Additionally, chemical and physical sterilization methods are performed during material processing. All of the abovementioned factors, including the biomaterial origin, harvesting compartment, processing, and purification technique and structure, influence the physical and chemical characteristics of the biomaterial; such as porosity, thickness, surface characteristics, polarization, and hydrophobicity.

In clinical applications, the biomaterial is implanted in a surgically created wound.[5] The cellular reaction in response to biomaterials is induced by the interaction between the host tissue and the biomaterial-specific surface initially after its implantation in vivo.[24] The biomaterial-specific physicochemical characteristics are decisive for the induced cellular reaction, which influences their regenerative capacity. After biomaterial implantation, both the innate and adaptive immune systems are involved in a localized cellular reaction.[25] In a systematic research series, our group investigated the cellular reaction to different biomaterials in vivo using a standardized subcutaneous implantation model.[5] Some biomaterials induced only mononuclear cells, such as monocytes, leukocytes, lymphocytes, and macrophages. Other biomaterials additionally showed the formation of multinucleated giant cells (MNGCs). Although the investigated materials were of the same origin (xenogeneic; porcine) and composition (collagen), they did induce different cellular reactions. However, it is still unanswered whether the biomaterial origin specifies the induced cellular reaction after implantation or if there are other factors that must be taken into consideration. Additionally, the role of MNGCs within the implantation bed of biomaterials is still not fully understood.[26] Some studies have proven these cells to be foreign body cells,[27] other studies demonstrated their capacity to express highly proinflammatory signaling molecules.[28] Therefore, investigating the induced cellular reaction is crucial for aiding scientists and clinicians in determining the suitable clinical indications according to the biomaterial's specific characteristics. Thereby, the aim of the present study was to classify the cellular reaction to different polymeric biomaterials and BSMs in a standardized implantation model in vivo and outline the clinical consequence of the biomaterial-specific cellular reaction for the regeneration process.

Materials and Methods

Studied materials

The present retrospective study evaluated 13 polymeric biomaterials and 19 BSMs of different compositions and origins. The samples were obtained from the archive of FORM-lab (Frankfurt Orofacial Regenerative Medicine, Goethe University) to provide an overview of the cellular reaction in vivo and classify the biomaterials according to the induced cellular reaction. In the following section, the evaluated biomaterials are described.

Polymeric biomaterials

In this study, the following resorbable and nonresorbable biomaterials were analyzed.

Nonresorbable Materials

- Gore membrane: A synthetic, nonresorbable, expanded PTFE membrane that serves as a barrier during the application time and has to be removed after a defined period of time (W.L. Gore & Associates, Inc, Newark, Del).[8]
- Medipac: According to the manufacturer, a synthetic, nonresorbable, nonreinforced membrane manufactured using PTFE that has been shown to be pyrogen free. This material is sterilized by ethylene oxide gas (Medipac, Stavrochori, Greece).
- Tefguide: According to the manufacturer, a synthetic nonresorbable thin PTFE-based membrane that is inert and resistant to bacteria. The membrane has high stability and supports epithelialization (Curasan AG, Kleinostheim, Germany).

Resorbable Materials

- Silk fibroin: A xenogeneic, naturally derived membrane extracted from Bombyx mori cocoons according to a previously described manufacturing protocol, which results in a low porous 3-dimensional (3D) membrane with varied fiber arrangements.[23]
- Biogide (BG): A xenogeneic, thin, bilayered, non–cross-linked collagen type I/III membrane of porcine origin (skin). This membrane is purified by standardized manufacturing methods and sterilized using gamma irradiation. BG exhibits a thin, low porous compact layer that serves as a barrier to prevent soft tissue ingrowth while the second spongy layer includes a more porous 3D structure to promote bone regeneration (Geistlich Biomaterials, Wolhousen, Switzerland).[8]

- Mucograft (MG): A xenogeneic, bilayered collagen matrix, which consists of collagen type I/III (porcine derived). Standardized manufacturing processes are applied to prevent immunogenic reactions. Additionally, the membrane is sterilized by gamma irradiation, while chemical cross-linking is avoided. MG contains two layers with different porosities and thicknesses. The thin and low porous compact layer is extracted from the porcine peritoneum and offers elasticity to adapt to host defect margins. The spongy layer, which is derived from porcine skin, shows higher porosity. This layer should face the bone defect to promote cell integration and proliferation (Geistlich Biomaterials).[29]
- Mucoderm: A xenogeneic, thick, non–cross-linked membrane, which consists of elastin and collagen type I/III in a defined 3D arrangement. The membrane is derived from porcine dermis and purified by lyophilization and gamma radiation (Botiss Biomaterials, Berlin, Germany).[30]
- Collprotect: A xenogeneic, bilayered, cross-linked membrane that consists of elastin and collagen type I/III derived from porcine dermis. The extracted collagen is manufactured with a 3D architecture. The membrane is lyophilized and sterilized by gamma radiation (Botiss Biomaterials).[30]
- Bego Collagen Fleece: A xenogeneic, bilayered, non–cross-linked collagen, type I/III membrane obtained from porcine dermis. Processing methods, such as controlled purification, are performed. Additionally, the membrane is lyophilized and sterilized by gamma irradiation (BEGO Implant Systems, Bremen, Germany).[31]
- Bego Collagen Membrane: A xenogeneic, non–cross-linked stratified membrane from porcine pericardium. The extracted collagen type I/III undergoes lyophilization and sterilization by ethylene oxide gas (BEGO Implant Systems).[31]
- Creos Xenoprotect: A xenogeneic, biodegradable membrane consisting of interwoven collagen and elastin fibers of porcine origin (Nobel Biocare, Kloten, Switzerland).[32]
- Symbios Collagen Membrane Sr: A xenogeneic collagen membrane obtained from bovine tendon. The membrane consists mainly of collagen type I (Dentsply Implants, York, Pa).[33]
- OSSIX PLUS Membrane: A xenogeneic, porcine-derived resorbable membrane. The collagen type I used is extracted from porcine tendons. Sugar cross-linking is performed using GLYMATRIX technology to enhance its stability. Sterilization is achieved with ethylene oxide (Regedent, Zurich, Switzerland).[20]

BSMs

Different synthetic and natural bone substitute materials were analyzed in this study.

- Bio-Oss: A xenogeneic biomaterial of bovine origin (BG; Geistlich Biomaterials). Bone is obtained from cancellous bovine bone. Purification and processing methods include chemical and physical treatment to remove all organic remnants in addition to irradiation and thermal sintering at 300°C. The bone granules exhibit a porosity of 70%–75%[34] with a trabecular structure similar to the human bone structure.[35]
- Bego-Oss : A xenogeneic BSM biomaterial of bovine origin (Bego Implant Systems). It is thoroughly purified by different washing steps and sintered at 1250°C. The material consists of hydroxyapatite (HA) and exhibits a natural structure with an interconnecting pore system.[16]
- Cerasorb granules: A synthetic BSM comprising beta-tricalcium phosphate (β-TCP), (Curasan, Kleinostheim, Germany). Five modifications of this biomaterial were analyzed using different granule morphologies and sizes as follows: A, polygonal morsels (500–1000 μm); B, polygonal morsels (150–500 μm); C, round granules (500–1000 μm); D, round granules (50–150 μm); E, polygonal morsels (63–250 μm).[36]
- BoneCeramic: A synthetic BSM comprising HA (60%) and β-TCP (40%) (Strauman, Freiburg, Germany). Two materials of the same chemical composition and different sizes were analyzed: A, 500–1000 μm; B, 400–700 μm.[37]
- BONITmatrix: A synthetic BSM comprising β-TCP, HA, and siliciumdioxid (DOT, Rostock, Germany). The components are interconnected with collagen and exhibit a porosity of 60%–80%.[38]
- NanoBone: A synthetic HA-based BSM (Artoss, Rostock, Germany). The particulated biomaterial consists of nanocrystalline HA (76%) and siliciumdioxid (24%) embedded in a matrix of silica gel. The granules have a porosity of 80% with an average size of 0.6 mm.[39]
- Ceramics: Three experimental ceramic BSMs were tested: (a) pure HA, (b) pure TCP, and (c) a combination of HA (60%) and TCP (40%). The granule sizes were 100–350 μm for all groups.
- CERASORB Paste: An injectable synthetic BSM (Curassan). This biomaterial comprises small-sized β-TCP granules (<63 mm) (30%) embedded in an organic matrix consisting of methylcellulose and sodium hyaluronate (70%).[40]
- FRIOS ALGIPORE: A phycogeneic BSM derived from red algae. The BSM is mainly HA based with a granule mean size of 0.3–2.0 mm (Dentsply Implants).[18]
- Hypro-Oss: A xenogeneic, bovine-derived BSM. The material comprises 30% atelocollagen type I and 70% HA. This BSM is not sintered. The granule size is between 0.5 and 1 mm (Bioimplon, Giessen, Germany).[41]

Subcutaneous implantation model in Wistar rats and CD-1 mice

This study provides a retrospective analysis of samples from the database of FORM-lab (Frankfurt Orofacial Regenerative Medicine), the Research Laboratory of the Department of Oral, Maxillofacial and Plastic Facial Surgery, Goethe University, Frankfurt, Germany. All included samples were obtained during systematic preclinical studies with ethical approval.

Description of the evaluated animal model

This study evaluated samples of biomaterial implantation in subcutaneous models of rats and mice, as previously described.[8,36]

In this model, biomaterials were implanted under the thin skin muscle panniculus carnosus in the subcutaneous tissue to evaluate the cellular reaction and inflammatory rate toward the biomaterials. Additional samples of animals that underwent

sham operation were used to evaluate the physiologic wound healing process without biomaterials. In total, 13 polymeric biomaterials and 19 BSMs of different compositions and origins were evaluated in this retrospective study. Each material group and control group were studied at 3, 15, and 30 days after implantation. Samples from 4 different animals per time point were evaluated for each material as described below.

Histologic preparation

Four slices per sample were stained using Mayer's hematoxylin and eosin (H&E) and Azan stain. The stained slides were evaluated by means of a light microscope (Nikon ECLIPSE 80i; Nikon, Tokyo, Japan) connected to a DS-Fi1/Digital camera (Nikon). This device was used to capture representative histologic pictures. The evaluation followed semiquantitative scores as described below.

Classification of biomaterials according to the induced cellular reaction

The induced cellular reaction in response to polymeric biomaterials and BSMs were classified systematically by means of semiquantitative scores to characterize the induced cellular reaction in relation to the biomaterial-specific physicochemical properties.

Semiquantitative analysis of the MNGC number in the biomaterials implantation bed

Semiquantitative analysis was performed to assess the number of MNGCs within each material per time point. Researchers evaluated the blinded histologic slides independently according to a score that was designed for this study (Table 1).

The evaluation was related to the respective time point to assess the increasing or decreasing tendency of the MNGC number within the implantation bed of each biomaterial. Four samples were evaluated for each time point and material. The results were tabulated as a tendency to increase or decrease in number of MNGCs over time.

Semiquantitative analysis of the vascularization rate in the biomaterials implantation bed

Semiquantitative analysis was performed to assess the vascularization rate of each material per time point compared with the previous time point starting at day 3. Researchers evaluated the blinded histologic slides independently according to a score that was designed for this study (Table 2). The evaluation focused only on the region of the implanted biomaterial (ie, the intergranular area in BSMs and the membrane/matrix area in polymeric materials). The results were tabulated as a tendency to increase or decrease the number of vessels over time.

Results

Classification of biomaterials according to the induced cellular reaction

The semiquantitative analysis of the cellular reaction over 30 days in response to biomaterials of different origins revealed several similarities and differences that allowed for the classification of biomaterials according to the induced cellular reaction by using a standardized implantation model. The subcutaneous implantation model in rats and mice was the main tool for the evaluation of medical devices in vivo. Polymeric biomaterials and BSMs were evaluated separately according to the MNGCs and vascularization scores.

Table 1

Semiquantitative score for the assessment of the multinucleated giant cells (MNGC) number

MNGC Score	Description
++	Number of MNGCs increased more than 50% compared with the previous time point
+	Number of MNGCs increased up to 50% compared with the previous time point
+/−	No obvious changes in the number of MNGCs compared with the previous time point
−	Number of MNGCs decreased up to 50% compared with the previous time point
−−	Number of MNGCs decreased more than 50% compared with the previous time point

Classification based on the MNGC score

The following classifications of polymeric biomaterials and bone substitute materials are described.

Polymeric Membranes and Matrices

Resorbable and nonresorbable polymeric membranes and matrices of different origins (porcine, bovine, and synthetic) were evaluated in this study. The observed kinetics of the induced MNGCs over 30 days allowed for their classification into 3 main classes. Interestingly, the MNGC induction did not correlate with the material origin (porcine, bovine, synthetic, etc) but was mainly associated with the material-specific physicochemical characteristics:

- Class I: Materials that induce no MNGCs at any time point. Two porcine-derived xenogeneic materials (Biogide and Mucograft) and one synthetic material (Medipac) showed no MNGC induction at any time point and were categorized in this class (Figures 1 and 2).

Table 2

Semiquantitative score for the assessment of the vascularization rate

Vascularization Score	Description
−	No vessels were observed within the biomaterial area
+/−	No obvious change in the vascularization rate
+	Low vascularization rate: number of vessels increased less than 25% compared with day 3
++	High vascularization: number of vessels increased up to 50% compared with day 3
+++	Highest vascularization: number of vessels increased more than 50% compared with day 3

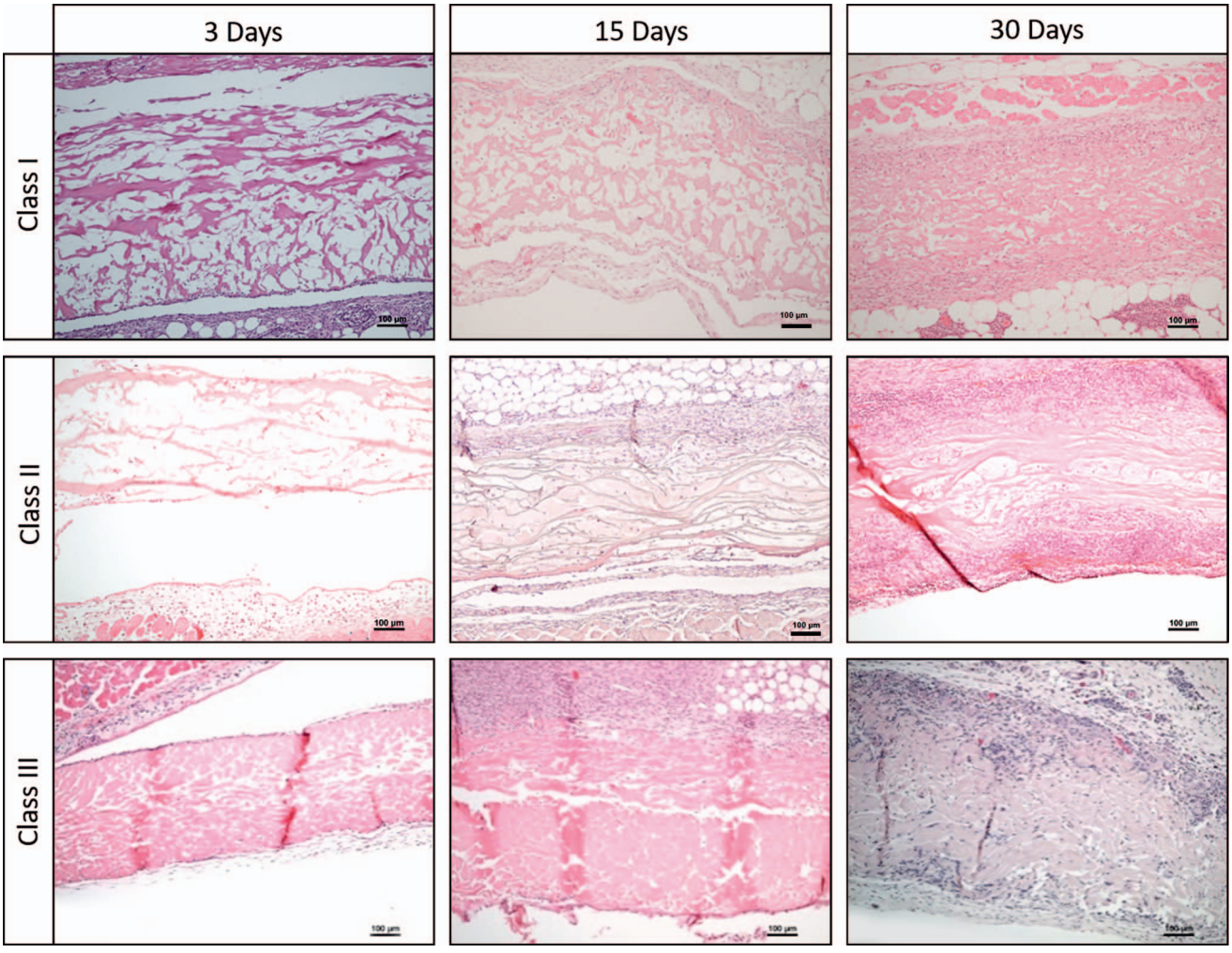

Figure 1. Representative histologic images for each class of the polymeric biomaterials over 30 days. All pictures were captured at ×100 magnification, with hematoxylin and eosin staining. Class I shows the cellular reaction to a porcine derived collagen matrix (Mucograft) that induced a mononuclear cell-based reaction and get integrated into the host tissue over 30 days. Class II shows the cellular reaction towards a bovine derived collagen membrane (Symbios membrane) that induced multinucleated giant cells (MNGCs) and underwent partial disintegration over 30 days. Class III shows the cellular reaction towards a porcine derived collagen membrane (Creos Xenoprotect) that induced an increasing number of MNGCs over 30 days and underwent total disintegration.

- Class II: Increasing tendency (3–15 days) and constant tendency (15–30 days). One synthetic membrane (Gore membrane), 2 porcine-derived collagen-based materials (Ossix Plus and Bego Collagen Membrane), and 1 bovine-derived collagen-based material (Symbios Collagen Membrane) induced MNGCs with increasing tendency (3–15) and a constant tendency between days 15 and 30 (Figures 1 and 2).
- Class III: Increasing tendency (3–30 days). Four porcine-derived collagen-based biomaterials (Bego Collagen Fleece, Creos Xenoprotect, Collprotect, and Mucoderm), 1 silk-based biomaterial (silk fibroin), and 1 synthetic membrane (Tefguide) induced MNGCs with increasing tendency from days 3 to 30 and were grouped in class III (Figures 1 and 2).

BSMs

This study evaluated BSMs of different origins (xenogeneic, synthetic, phycogeneic). Interestingly, different kinetics of the induced MNGCs were observed when comparing materials from the same origin (eg, xenogeneic [bovine]). Thereby, the observed cellular reaction did not depend on the material origin but on the physicochemical characteristics of the material (ie, porosity, surface characteristics, processing technique, polarity).

All materials induced MNGCs. However, the number of MNGCs over the observed time points differed markedly according to the analyzed material. Therefore, the kinetics of the MNGC numbers over 30 days were classified into 3 different patterns.

- Class I: Increasing tendency (3–15 days) and decreasing tendency (15–30 days). One bovine (Bio-Oss) and 2 synthetic BSMs (BONITmatrix, Cerasorb C) induced MNGCs with increasing tendency from days 3 to 15. The kinetics changed to a markedly decreasing tendency from days 15 to 30 (Figures 3 and 4).

Figure 2. The classification of polymeric biomaterials according to the cellular reaction.

- Class II: Materials inducing MNGCs with constant tendency over 30 days. Three synthetic BSMs (Cerasorb E, Bone-Ceramic A, and HA) and 2 bovine-derived xenogeneic BSMs (Bego-Oss and Hypro-Oss) showed an increasing tendency from days 3 to 15. The kinetics changed to a constant tendency from days 15 to 30. These materials were classified in class II (Figures 3 and 4).
- Class III: Materials inducing MNGCs with increasing tendency over 30 days. Seven synthetic BSMs (Cerasorb A, Cerasorb B, Cerasorb D, BoneCeramic, Cerasorb Paste, NanoBone, and tricalcium phosphate) and 1 phycogeneic BSM (Frios Algipore) induced MNGCs with continuously increasing tendency over 30 days and were classified in class III (Figures 3 and 4).

Control Group

In the control group, no biomaterial was implanted (sham operations), and no MNGCs were observed at any time point (data not shown).

Classification based on the vascularization score

The vascularization rate of polymeric biomaterials and bone substitute materials was evaluated according to the vascularization score.

Polymeric Membranes and Matrices

Two different patterns of vascularization were assessed, generating 2 categories in which the evaluated biomaterials were classified.

- Class I: Materials that underwent no vascularization at any time point. In 8 polymeric biomaterials (3 nonresorbable membranes [Gore Membrane, Tefguife, Medipac] and 5 collagen-based biomaterials with different origins [Biogide, Mucograft, Ossix Plus, Symbios collagen membrane, and Bego collagen membrane]), no vessels were observed within the biomaterial body at any time point. These materials were categorized as class I (Figures 5 and 6).
- Class II: Materials that undergo increasing vascularization over 30 days. A second group of biomaterials (4 collagen-based biomaterials of different origins [Bego Collagen Fleece, Collprotect, Creos Xenoprotect, Mucoderm] and 1 silk-based biomaterial) induced vessels with increasing tendency that were observed within the bodies of the biomaterials. These materials were categorized as class II (Figures 5 and 6).

BSMs

According to the vascularization score, 2 different vascularization patterns were observed in the group of BSMs based on the vascularization tendency over 30 days.

- Class I: Materials that undergo increasing vascularization over 30 days. Seven synthetic BSMs (BoneCeramic B, Cerasorb Pase, Cerasorb A, Cerasorb B, Cerasorb D, Nano-Bone, and tricalcium phosphate) and 1 phycogeneic BSM (Frios Algipore) showed an increasing vascularization tendency over 30 days and were categorized in class I (Figures 6 and 7).

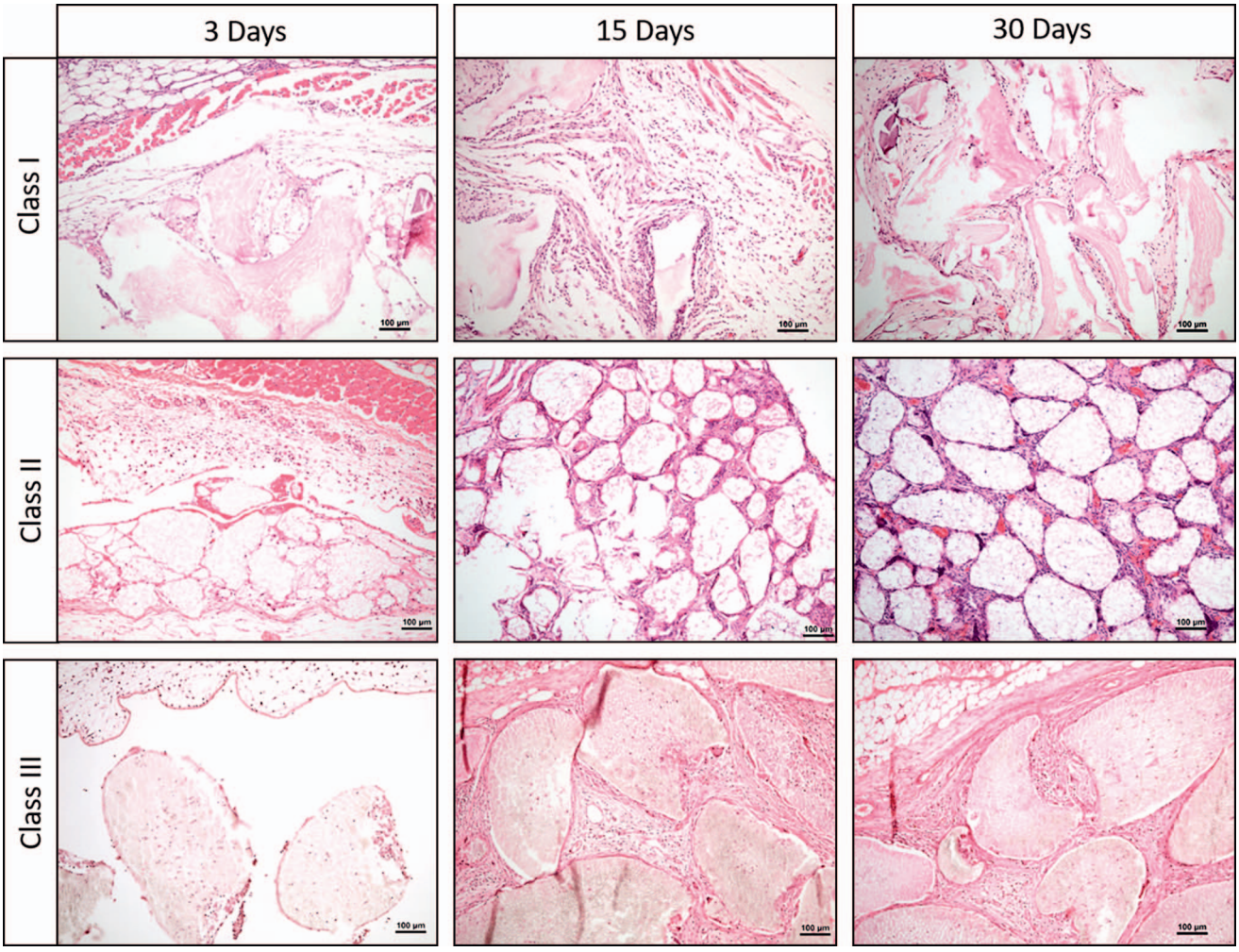

Figure 3. Representative histologic images for each class of the bone substitute biomaterials over 30 days. All pictures were captured at ×100 magnification, with hematoxylin and eosin staining. Class I shows the cellular reaction to a bovine derived BSM (Bio-Oss) that induced an initial number of multinucleated giant cells (MNGCs) that decreased towards day 30. Class II shows the cellular reaction towards synthetic bone substitute material (BSM; Cerasorb A) that induced MNGCs with constant number over 30 days. Class III shows the cellular reaction towards a phycogenic BSM (Frios Algipore) that induced an increasing number of MNGCs over 30 days.

- Class II: Materials that show a constant vascularization rate over 30 days. Class II included 5 synthetic BSMs (BONITmatrix, BoneCeramic A, Cerasorb E, Cerasorb C, and HA) and 3 xenogeneic BSMs of bovine origin (Bego-Oss, Bio-Oss, Hypro-Oss). These materials induced an initial increase in vascularization from days 3 to 15 and showed a mainly constant tendency between days 15 and 30 (Figures 6 and 7).

Control Group

In the control group, no biomaterials were implanted (sham operation). The vascularization rate showed a slight increasing tendency over 30 days.

Consequences of the biomaterial-induced cellular reaction type

Each induced cellular reaction had different consequences for the biomaterials and thereby the regeneration patterns of the biomaterials. Both polymeric biomaterials and BSMs showed characteristic consequences based on the induced cellular reaction, as classified in the previous section.

Polymeric biomaterials

Resorbable and nonresorbable polymeric biomaterials were analyzed in this study. The consequences of the induced cellular reaction are described and illustrated for each group as follows.

Resorbable Polymeric Biomaterials

In the group of resorbable polymeric biomaterials, 3 different reactions were observed and classified according to the MNGC score:

1. Integration by inducing a mononuclear cell–based reaction and the absence of MNGCs (class I according to the MNGC score),

Biomaterial	Composition	Origin	Appearance	Size (µm)	Intergranular Porosity (%)	Sinter Temperature (°C)
Bio-Oss®	Hydroxyapatite (Cancellous bone)	Bovine	Polygon	250-1000	300	N/A
BONITmatrix®	Hydroxyapatite Beta-tricalcium phosphate Silicon dioxide Interconnected with collagen	Synthetic	Scaffold	N/A	200	1200
Cerasorb® C	Beta-tricalcium phosphate	Synthetic	Round	500-1000	1300	700

Biomaterial	Composition	Origin	Appearance	Size (µm)	Intergranular Porosity (%)	Sinter Temperature (°C)
Hypro-Oss®	Atelo-collagen type I (30%) Hydroxyapatite (70%)	Bovine	Polygon	500-1000	N/A	N/A
Bego-Oss®	Hydroxyapatite (cancellous bone)	Bovine	Polygon	500-1000	70-80	1200
BoneCeramic® A	Hydroxyapatite (60%) Beta-tricalcium phosphate (40%)	Synthetic	Polygon	500-1000	N/A	700
Cerasorb® E	Beta-tricalcium phosphate	Synthetic	Polygon	36-250	25	1300
Experimental Product	Hydroxyapatite (60%) Beta-tricalcium phosphate (40%)	Synthetic	Round	100-350	50	1300
Experimental Product	Hydroxyapatite	Synthetic	Round	100-350	60-80	1300

Biomaterial	Composition	Origin	Appearance	Size (µm)	Intergranular Porosity (%)	Sinter Temperature (°C)
Frios® Algipore®	Hydroxyapatite	red algae	Cylinder	1000-2000	N/A	N/A
BoneCeramic® B	Hydroxyapatite (60%) Beta-tricalcium phosphate (40%)	synthetic	Polygon	400-700	N/A	N/A
Cerasorb® paste	Beta-tricalcium phosphate granules (30%) Methylcellulose and sodium hyaluronate (70%)	synthetic	Paste	63	N/A	1000
Cerasorb® A	Beta-tricalcium phosphate	synthetic	Polygon	500-1000	65	1300
Cerasorb® B	Beta-tricalcium phosphate	synthetic	Polygon	150-500	65	1300
Cerasorb® D	Beta-tricalcium phosphate	synthetic	Polygon	50-150	35	1300
NanoBone®	Nanocrystalline hydroxyapatite (76%) Silicon dioxide (24%) Matrix of silica gel	synthetic	Fir cone	600-2000	60-80	1300
Experimental Product	Beta-Tricalciumphosphate	synthetic	round	100-350	60-80	1300

Figure 4. The classification of bone substitute materials according to the cellular reaction.

2. Partial disintegration by inducing MNGCs in a constant and persistent tendency (class II according to the MNGC index), and
3. Disintegration by inducing a continual increasing number of MNGCs (class III according to the MNGC score).

The consequences of the induced reaction in each class are described and illustrated below.

Integration by inducing a mononuclear cell–based reaction and the absence of MNGCs

Class I according to the MNGC score included biomaterials that induced only mononuclear cells such as monocytes, macrophages, lymphocytes, and fibroblasts. Two resorbable collagen-based biomaterials were categorized in class I for both integration processes. First, an initial reaction (day 3) characterized by

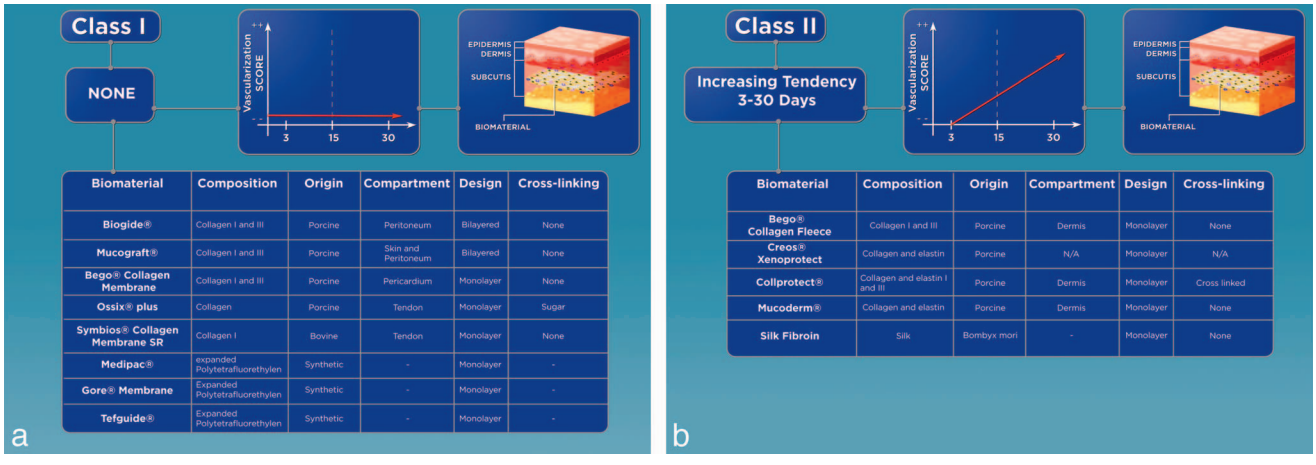

Biomaterial	Composition	Origin	Compartment	Design	Cross-linking
Biogide®	Collagen I and III	Porcine	Peritoneum	Bilayered	None
Mucograft®	Collagen I and III	Porcine	Skin and Peritoneum	Bilayered	None
Bego® Collagen Membrane	Collagen I and III	Porcine	Pericardium	Monolayer	None
Ossix® plus	Collagen	Porcine	Tendon	Monolayer	Sugar
Symbios® Collagen Membrane SR	Collagen I	Bovine	Tendon	Monolayer	None
Medipac®	expanded Polytetrafluorethylen	Synthetic	-	Monolayer	-
Gore® Membrane	Expanded Polytetrafluorethylen	Synthetic	-	Monolayer	-
Tefguide®	Expanded Polytetrafluorethylen	Synthetic	-	Monolayer	-

Biomaterial	Composition	Origin	Compartment	Design	Cross-linking
Bego® Collagen Fleece	Collagen I and III	Porcine	Dermis	Monolayer	None
Creos® Xenoprotect	Collagen and elastin	Porcine	N/A	Monolayer	N/A
Collprotect®	Collagen and elastin I and III	Porcine	Dermis	Monolayer	Cross linked
Mucoderm®	Collagen and elastin	Porcine	Dermis	Monolayer	None
Silk Fibroin	Silk	Bombyx mori	-	Monolayer	None

Figure 5. The vascularization classes of the polymeric biomaterials.

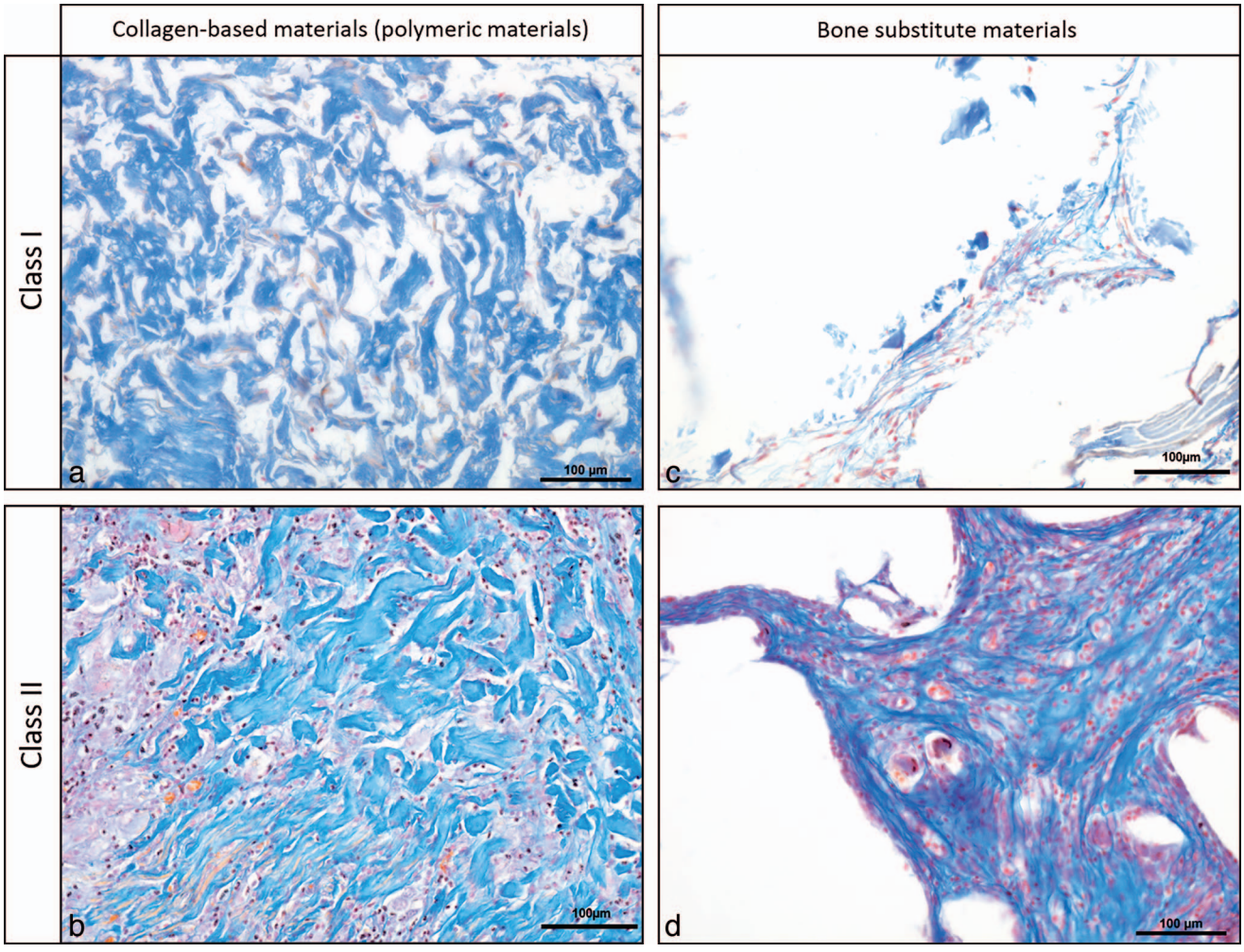

Figure 6. Representative histologic images of the vascularization pattern on day 30. (a) Mucograft showed no vessel formation within the membrane (class I). (b) Creos Xenoprotect represents class II and shows vessel formation within the membrane central region (arrows). (c) Mild vascularization in Bio-Oss as a representative biomaterial for class I. (d) High vascularization in Cerasorb A (class II) shows vessel formation within the intergranular area (arrows). All pictures were captured at ×200 magnification, with azan staining.

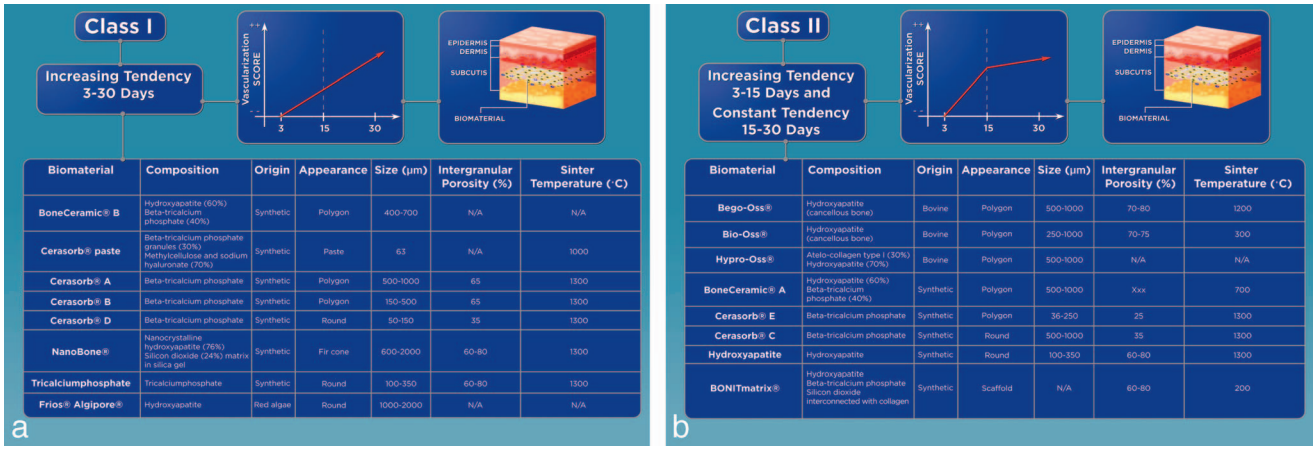

Biomaterial	Composition	Origin	Appearance	Size (µm)	Intergranular Porosity (%)	Sinter Temperature (°C)
BoneCeramic® B	Hydroxyapatite (60%) Beta-tricalcium phosphate (40%)	Synthetic	Polygon	400-700	N/A	N/A
Cerasorb® paste	Beta-tricalcium phosphate granules (30%) Methylcellulose and sodium hyaluronate (70%)	Synthetic	Paste	63	N/A	1000
Cerasorb® A	Beta-tricalcium phosphate	Synthetic	Polygon	500-1000	65	1300
Cerasorb® B	Beta-tricalcium phosphate	Synthetic	Polygon	150-500	65	1300
Cerasorb® D	Beta-tricalcium phosphate	Synthetic	Round	50-150	35	1300
NanoBone®	Nanocrystalline hydroxyapatite (76%) Silicon dioxide (24%) matrix in silica gel	Synthetic	Fir cone	600-2000	60-80	1300
Tricalciumphosphate	Tricalciumphosphate	Synthetic	Round	100-350	60-80	1300
Frios® Algipore®	Hydroxyapatite	Red algae	Round	1000-2000	N/A	N/A

Biomaterial	Composition	Origin	Appearance	Size (µm)	Intergranular Porosity (%)	Sinter Temperature (°C)
Bego-Oss®	Hydroxyapatite (cancellous bone)	Bovine	Polygon	500-1000	70-80	1200
Bio-Oss®	Hydroxyapatite (cancellous bone)	Bovine	Polygon	250-1000	70-75	300
Hypro-Oss®	Atelo-collagen type I (30%) Hydroxyapatite (70%)	Bovine	Polygon	500-1000	N/A	N/A
BoneCeramic® A	Hydroxyapatite (60%) Beta-tricalcium phosphate (40%)	Synthetic	Polygon	500-1000	Xxx	700
Cerasorb® E	Beta-tricalcium phosphate	Synthetic	Polygon	36-250	25	1300
Cerasorb® C	Beta-tricalcium phosphate	Synthetic	Round	500-1000	35	1300
Hydroxyapatite	Hydroxyapatite	Synthetic	Round	100-350	60-80	1300
BONITmatrix®	Hydroxyapatite Beta-tricalcium phosphate Silicon dioxide interconnected with collagen	Synthetic	Scaffold	N/A	60-80	200

Figure 7. The vascularization classes of bone substitute materials.

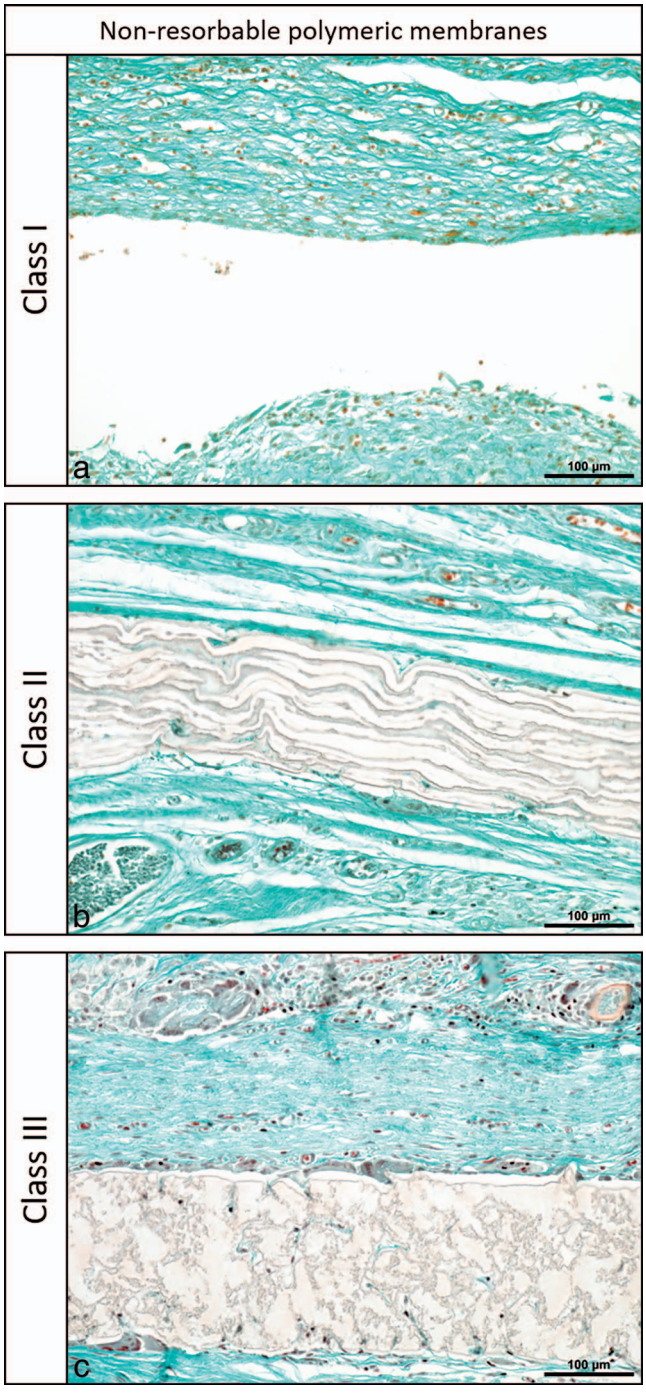

Figure 8. Representative histochemical images of nonresorbable biomaterials and capsule formation on day 30. (a) Class I (Medipac) shows a loose reticular capsule. (b) Class II (Gore Membrane) shows a rather woven connective tissue. (c) Class III (Tefguide) shows a thick dense capsule. All pictures were captured at ×100 magnification, with Masson Goldner staining.

mononuclear cells took place. In this early phase, mainly macrophages, fibroblasts, and some lymphocytes were observed. Then, stepwise cell penetration in the superficial layers of the membranes was observed (days 10–15). Here again, only a mild accumulation of the mononuclear cells was part of the reaction. Obviously, the membranes acted as a scaffold, allowing the cells to adhere between the collagen fibers without causing a breakdown. Subsequently, connective tissue formation (day 30) within and around the membrane was typical for this phase of the reaction. At this time point, the mononuclear cells continued penetrating the membranes. The collagen-based biomaterials were well integrated within the newly formed connective tissue. A merge of the xenogeneic collagen-based biomaterial and the newly formed connective tissue of the host occurred, leading to the integration of the biomaterial within the host tissue. The biomaterial maintained its native structure and integrity. Additionally, no vessel formation at the integration region was observed at any time point (Figure 9a).

Partial disintegration by inducing MNGCs with a constant and persistent tendency

The biomaterials that induced a constant and persistent tendency of MNGC number from days 15 to 30 were categorized in class II according to the MNGC index. These biomaterials, including 2 porcine-derived collagen-based biomaterials and 1 bovine-derived collagen-based biomaterial, showed similar cellular reactions over 30 days. Initially, only mononuclear cells were observed on the biomaterial surfaces. On days 15 and 30, MNGCs were observed on the surfaces of the biomaterials. However, MNGCs did not penetrate the body of the biomaterials during the observed time points in any of the biomaterials categorized here. Therefore, the membrane preserved its initial structure and integrity. No signs of material breakdown were observed. Additionally, no vessel formation was found within the central region of the biomaterials at any time point (Figure 9b).

Disintegration by inducing an increasing number of MNGCs

Four porcine-derived collagen-based biomaterials and 1 silk-based biomaterial showed very similar tissue reactions, which led to their categorization in class III according to the MNGC index. These materials underwent disintegration as a consequence of inducing an increasing number of MNGCs. This process was similar to the initial reaction (day 3) observed in the case of integration. This early stage of the reaction showed mononuclear cells represented by macrophages, fibroblasts, and leukocytes. Thereafter, enhanced cell accumulation was observed in all cases, forming a wall of inflammatory cells on both sides of the membrane. This phase was then followed by (day 15) the fusion of macrophages with MNGCs. These cells started to invade the membranes (day 30) from both sides, forming roads for mononuclear cells and allowing the premature ingrowth of connective tissue and the formation of granulation tissue within the membrane. Here, signs of membrane breakdown were seen in most of the membranes. Finally, a membrane breakdown with MNGC accumulation was observed in all membranes, which induced an increase in the number of MNGCs. Moreover, the occurrence and accumulation of MNGCs was accompanied by increased vascularization within the central region of the biomaterials (Figure 9c).

Nonresorbable polymeric materials

Three nonresorbable polymeric materials were analyzed in this study. Interestingly, although all materials are PTFE based,

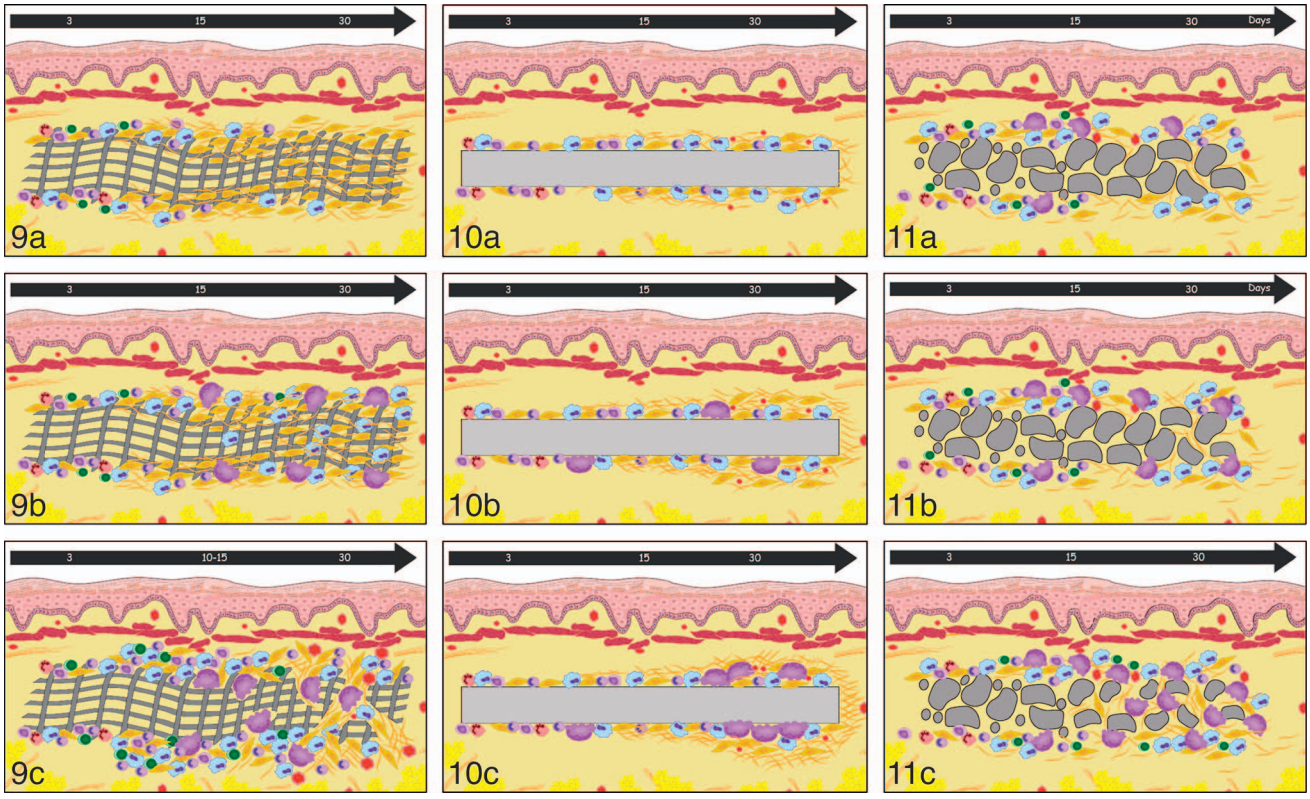

Figures 9–11. Figure 9. Illustrative artwork of the processes of integration and disintegration in polymeric biomaterials. (a) The process of integration by the absence of multinucleated giant cells (MNGCs) (class I). (b) Partial disintegration by a constant number of MNGCs (class II). (c) Disintegration by an increasing number of MNGCs (class III). **Figure 10.** Illustrative artwork of the process of encapsulation in nonresorbable biomaterials as a consequence of the induction of MNGCs during the foreign body reaction. (a) Loss of the reticular capsule by the induction of only mononuclear cells (class I). (b) Partial encapsulation by the induction of a constant number of MNGCs (class II). (c) Encapsulation by the induction of an increasing number of MNGCs (class III). **Figure 11.** Illustrative artwork of the process of granule integration and degradation as a consequence of the induction of MNGCs during the foreign body reaction. (a) Integration of the granules by inducing a decreasing number of MNGCs. (b) Partial degradation by inducing a constant number of MNGCs (class II). (c) Rapid degradation by inducing an increasing number of MNGCs (class III).

different cellular reactions were observed. According to the MNGC score, the 3 PTFE-based membranes were categorized into 3 different classes. Therefore, different consequences based on the induced cellular reaction were observed:

1. Loose reticular capsule formation by inducing only mononuclear cells and the absence of MNGCs (class I according to the MNGCs score),
2. Partial encapsulation by inducing a constant number of MNGCs over 30 days (class III according to the MNGCs score), and
3. Dense and thick capsule formation by inducing an increase in the number of MNGCs over 30 days (class III according to the MNGC score).

Loose reticular capsule formation by inducing only mononuclear cells and the absence of MNGCs

One PTFE-based membrane (Medipac) induced only mononuclear cells over 30 days. No MNGC formation was observed at any time point (class I according to the MNGC score). Initially, mononuclear cells started accumulating on the biomaterial surface (day 3). More mononuclear cells (ie, monocytes, macrophages, lymphocytes, and fibroblasts) were observed on day 15. Over time, a rather loose reticular capsule was formed around the biomaterials (day 30). No vessels or cellular penetration was observed within the body of the biomaterials at any time point (Figures 8 and 10a)

Encapsulation by inducing a constant number of MNGCs

Another PTFE-based membrane (Gore Membrane) was classified as class II according to the MNGC score. This membrane induced MNGCs starting on day 15. However, no increasing tendency of the MNGC number was observed between days 15 and 30. In contrast, the number of induced MNGCs showed a rather constant tendency. Thereby, a fibrous capsule that included only some MNGCs on day 30 surrounded the membrane. No vessels were observed within the body of the biomaterials at any time point (Figures 8 and 10b).

Dense and thick capsule formation by inducing an increasing number of MNGCs

In the case of the nonresorbable PTFE-based membrane (Tefguide) that was categorized as class III (according to the MNGC index), a specific tissue response was observed. The

initial reaction (day 3) by mononuclear cells was similar to the process of integration and disintegration. MNGCs were detectable on both surfaces of the membrane (day 15). Remarkably, no infiltration of the membrane was recognizable in this phase of the reaction. However, encapsulation was observed in the late reaction period (day 30), caused by the formation of vascularized connective tissue. At this point in time, the membrane remained resistant. Although the rate of the MNGCs slightly increased, no breakdown of the membrane or cell penetration of any kind was revealed at any phase of the reaction (Figures 8 and 10c).

BSMs

Various synthetic and natural BSMs of different origins were analyzed in this study. According to the induced cellular reaction (MNGC score), the BSMs were classified into 3 groups. The number and tendency of the induced MNGCs correlated with the biomaterial degradation and the rate of vascularization. Thereby, 3 scenarios were observed:

1. Integration by inducing MNGCs then followed by a decreasing number (class I according to the MNGC score),
2. Intermediate reaction by inducing and maintaining a constant number of MNGCs (class II according to the MNGC score), and
3. Rapid degradation by inducing MNGCs then followed by an increasing number of MNGCs (class III according to the MNGC score).

These scenarios are described and illustrated in the following.

Integration by inducing MNGCs with decreasing tendency

Two synthetic and one bovine BSM were classified as class I according to the MNGC score. These materials showed an initial reaction that was based on mononuclear cells only. On day 15, some MNGCs were observed. However, their number markedly decreased on day 30. No obvious biomaterial degradation was observed on day 30 compared with day 3. These materials were well integrated within the implanted region and showed no increasing tendency of vascularization. The intergranular area was not extremely invaded by connective tissue on day 30 (Figure 11a).

Partial Disintegration by Inducing a Constant Number of MNGCs

Three synthetic and 2 bovine-derived BSMs were classified as class II according to the MNGC score. This group showed an intermediate reaction by inducing a constant number of MNGCs between days 15 and 30. Therefore, within the observation time period, no obvious degradation was recorded in this group when comparing the granule sizes from days 3 to 30. This group also induced a constant tendency of vascularization. The intergranular area was filled with connective tissue from the peri-implantation region (Figure 11b).

Rapid Degradation by Inducing an Increasing Number of MNGCs

Class III, which included 7 synthetic BSMs and 1 phycogeneic BSM, induced a high number of MNGCs over the study period that caused rapid degradation and allowed the peri-implantation of connective tissue into the intergranular area. Therefore, the induction of a high number of MNGCs in this case was associated with biomaterial degradation and an increasing tendency of vascularization (Figure 11c).

Discussion

In biomaterials science, the development of manufacturing techniques and the variety of sources that are used for biomaterial fabrications have necessitated the need for a classification system. The classification system(s) would provide clinicians and researcher with an overview of existing and new biomaterials that would aid in assessing the physicochemical characteristics and properties of the various biomaterials. Existing classifications focus mainly on the absorbability and origin or harvesting species/region.[8] These classification systems are useful for evaluating the biomaterial compositions and manufacturing characteristics.[43] However, recent studies have shown that biomaterials of the same origin (ie, xenogeneic) may induce different types of cellular reactions in vivo.[8] Similarly, biomaterials of different origins (ie, xenogeneic and synthetic) may induce the same cellular reaction in vivo.[5] Based on these observations, the in vivo cellular reaction to biomaterials is of great clinical importance, as it may provide information about the regeneration pattern induced by a specific biomaterial.[44–46] Based on these hypotheses, and the fact that in the last decade there has been an influx of multiple new biomaterials into the market place, there is now a need for a new classification system that evaluates biomaterials from a clinical response perspective. Therefore, the present study aimed to define a new classification system based on the induced cellular reaction to facilitate clinical decisions according to the patient-specific clinical indication.

The present results show that it is possible to classify biomaterials according to the induced cellular reaction in vivo. Thereby, the first class (class I) included materials that induced only mononuclear cells, such as macrophages, lymphocytes, and fibroblasts. Based on the biomaterial characteristics that were categorized in this class (2 porcine-derived collagen-based biomaterials and 1 nonresorbable PTFE-based membrane), the induced cellular reaction obviously did not depend on the biomaterial's origin.

Interestingly, the same was shown for the next 2 classes that illustrated materials that evoke MGNCs in a constant tendency over 30 days (class II) and materials that attract MNGCs in a continually increasing number over 30 days (class III). The formation of MGNCs, their numbers, and persistence kinetics depended on biomaterial-specific physicochemical properties, such as chemical composition, thickness, stiffness, hydrophobicity, porosity, shape, and size. For example, 8 polymeric collagen-based biomaterials were evaluated in this study. Although all these materials were of xenogeneic origin and derived from the same species (ie, porcine tissue), different inflammatory patterns were observed. Only 2 of the 8 evaluated collagen-based biomaterials elicited a mononuclear cell–based reaction (class I), whereas the other 6 induced MNGCs with different tendencies.

Consequently, polymeric biomaterials that were categorized in class I were associated with slow degradation and no vascularization within the biomaterial body. In contrast, the

attraction of a high number of MNGCs with a continually increasing tendency (class III) was accompanied by a rapid fragmentation of the biomaterial (ie, biomaterial disintegration and a high rate of vascularization). Interestingly, class II, which induced a constant number of MNGCs, did not undergo disintegration. These findings highlight that the composition and surface characteristics of this material group may delay the disintegration reaction by MNGCs. However, this study is limited to 30 days; therefore, this material group may undergo a similar pattern as with class III materials at a later time point.

A similar observation was true for the 3 evaluated PTFE-based membranes that illustrated 3 different cellular reactions, although these membranes have the same chemical composition.

When evaluating the results of BSMs, it became obvious that when considering the cellular reaction as a parameter for classification of biomaterials, the initial origin (eg, natural or synthetic) is not an important factor responsible for the induced cellular reaction. This finding is evidenced in all classes that were defined according to the MNGC score. Class I included 2 synthetic and 1 xenogeneic BSM, and all 3 materials induced a decreasing tendency of MNGCs. Similarly, classes II and III include materials of different origins (synthetic and natural) that had a similar cellular reaction. The present results illustrated that 3 bovine-based BSMs induce different cellular reactions, although they are of the same origin. The relevant difference in their processing technique is the sintering temperature. The low-temperature sintered biomaterial induced MNGCs with decreasing tendency over 30 days (class I), whereas the high temperature sintered BSM induced MNGCs with a constant tendency that determined a completely different regeneration pattern. Thus, the processing technique seems to have an extensive impact on the biomaterial and surface characteristics that directly attract the cells in the implantation bed. Another example is provided when examining different synthetic granules (Cerasorb) comprising the same chemical formula (TCP) but with different granule sizes and morphologies. This parameter (size and morphology) had an extreme impact on the biomaterial-induced cellular reaction, so that some of the granules induced MNGCs with increasing tendency (eg, Cerasorb A: class III). Other granules of the same chemical composition induced a different reaction and induced either MNGCs with a constant tendency (Cerasorb E: class II) or a decreasing tendency (Cerasorb C: class I), and this result was similar to the cellular reaction induced by the natural bovine-derived BSM.

The physicochemical characteristics of biomaterials are created during manufacturing (sintering, cross-linking, sterilization, chemical treatment).[16,19,20] Although naturally derived biomaterials are not synthetically manufactured, each biomaterial undergoes different processing, purification, and sterilization methods.[19,47]

These observations underline the hypothesis that the surface characteristics and protein absorbance capacity determine the induced formation of MNGCs.[48] This hypothesis is supported by a previous in vivo study that demonstrated the correlation between surface hydrophilicity and the adhesion of macrophages, suggesting that hydrophilic surfaces prevent macrophage adhesion and lead to increased macrophage apoptosis.[49] In this case, this phenomenon reduces the fusion of macrophages into MNGCs.[49] Therefore, the fusion of MNGCs is dependent on specific adhesion proteins, such as integrin β 1 and 2.[50] In this context, the different manufacturing, purification, processing, and sterilization techniques for collagen-based biomaterials may be the reason for changes in the biomaterial surfaces that provoke the formation of MNGCs in some collagen-based biomaterials.[19]

In terms of the bone substitute materials, the formation of MNGCs was related most notably to the chemical composition of the biomaterial and other unidentified factors.[49,51] A recent in vivo study evaluated different shapes of poly(L-lactide-co-D/L-lactide) implants using a subcutaneous implantation model in rats. The results were in accordance with our results and showed that the highest number of MNGCs was induced in response to the mesh shape compared with the membrane shape. However, smaller differences were observed when the mesh shape was maintained, and the surface was either coated or not with plasma-polymerized allylamine.[52] A further in vivo study evaluated the surface processing of β-TCP granules using either plasma or purified fibrin. The differently processed biomaterials were implanted using a subcutaneous implantation model in vivo. The results showed that altered processing led to the induction of different MNGC phenotypes. In this context, plasma-processed granules induced cathepsin-positive MNGCs and fibrin-processed granules induced cathepsin-negative MNGCs.[53] These data demonstrated that processing the surface can be used to stimulate MGNCs to adapt to specific phenotypes. However, to date, little is known about the MNGC phenotypes and their roles in the regeneration process.

The present study demonstrated the following: biomaterials that induce only mononuclear cells preserve their native structure over a rather long time period and become integrated into the host tissue, whereas biomaterials that induce MNGCs with increasing tendency become disintegrated, which is evidenced by the fragmentation of the biomaterials and the loss of the native structure, followed by premature degradation.

When transferring the data presented here to a clinical situation, it must be taken into consideration that the GBR concept is based on the use of so-called barrier membranes that should separate the soft tissue from the bony defect to permit bone regeneration and prevent soft tissue ingrowth.[14] Taking these requirements together with the results presented herein, it becomes obvious that resorbable biomaterials, in general, cannot be considered as a barrier because at some time point, it is expected that these biomaterials will degrade. Therefore, based on the present results, resorbable polymeric biomaterials, especially those that induce a mononuclear cell–based reaction and become integrated, may be defined as functional barriers. However, biomaterials that induce MNGCs and undergo disintegration may not comply with the requirement of GBR for a long time period. Therefore, the results of the present study outlined that the biomaterial source (eg, porcine-derived collagen) does not determine its regenerative capacity. Therefore, clinicians should pay more attention to the biomaterial-induced cellular reaction and the

subsequent degradation pattern when considering the application of biomaterials for specific clinical indications.

Rapidly degradable BSMs may be counterproductive with respect to the long-term preservation of the augmented bone, especially in atrophic bone. In this case, after biomaterial degradation, the augmentation area may return to its atrophic condition because of the lack of biological and mechanical stimuli. Therefore, slowly degradable biomaterials, such as BSMs of class I, may be beneficial for application in atrophic bone as these materials become well integrated into the augmentation area and build a so-called "hybrid bone" consisting of the patients' own newly formed bone and the granules of the applied BSMs.[54] These findings were consistent with recent clinical studies that evaluated 2 different biomaterials in a split-mouth clinical study. The evaluated biomaterials were synthetic and xenogeneic. The histologic analysis showed that a high number of MNGCs was associated with a higher degradation of the biomaterial compared with materials with limited induction of MNGCs.[1,54,55]

However, other clinical indications, such as socket preservation after freshly extracted teeth in young patients who do not have bone atrophy, may require the use of rapidly degradable biomaterials. In this case, BSMs should initially support the regeneration process and then become degraded. In such clinical scenarios, BSMs of class II and class III may be more suitable.[44]

These observations enhance the importance of understanding the cellular reaction to biomaterials to assess the regenerative capacity and define the suitable clinical indication for each biomaterial class. Based on these data, further controlled clinical studies are needed to verify the proposed concepts and outline potential benefits to maximize clinical results.

Special interest has been directed toward biomaterial-induced MNGCs and their roles in the biomaterial-based regeneration process. A recent histologic study in human biopsies proved that biomaterial-induced MNGCs express proinflammatory molecules rather than anti-inflammatory signaling molecule.[28] However, until recently, little was known about the polarization of MNGCs and the type of MNGCs that can be induced by which biomaterial. Therefore, further studies in this field are of great interest for both biomaterials scientists and clinicians. Furthermore, it must be critically evaluated whether the use of biomaterials that induce MNGCs is beneficial for clinical application or whether clinicians should concentrate on the application of biomaterials that induce a physiologic reaction based on mononuclear cells in combination with further tissue engineering strategies to manage the clinical situation. Therefore, systematic and controlled clinical studies are highly needed to evaluate these concepts.

Conclusion

This study showed that it is possible to classify biomaterials according to the induced cellular reaction in a novel classification system for polymeric biomaterials and BSMs. The present study outlined the relevance of the biomaterial-induced cellular reaction. Furthermore, the induction of MNGCs depended on the biomaterial-specific physicochemical properties and not on the biomaterial origin (synthetic vs natural). This novel classification system provides clinicians with a tool to assess the regeneration pattern of biomaterials and aid in one's critical thinking regarding the suitability of a product for an intended clinical situation.

Abbreviations

BG: BioGuide
BSM: bone substitute material
GBR: guided bone regeneration
GTR: guided tissue regeneration
H&E: hematoxylin and eosin
HA: hydroxyapatite
MG: Mucograft
MGNC: multinucleated giant cells
PCL: polycaprolactone
PLA: polylactic acid
PLGA: poly(lactic-co-glycolic acid)
PTFE: polytetrafluorethylene
β-TCP: beta-tricalcium phosphate

Acknowledgment

The authors thank Verena Hoffmann for excellent technical support in histology.

Note

The authors declare no conflicts of interest.

References

1. Ghanaati S, Barbeck M, Lorenz J, et al. Synthetic bone substitute material comparable with xenogeneic material for bone tissue regeneration in oral cancer patients: first and preliminary histological, histomorphometrical and clinical results. *Ann Maxillofac Surg*. 2013;3:126–138.

2. Lorenz J, Kubesch A, Korzinskas T, et al. TRAP-positive multinucleated giant cells are foreign body giant cells rather than osteoclasts: results from a split-mouth study in humans. *J Oral Implantol*. 2015;41:e257–e266.

3. Lorenz J, Blume M, Barbeck M, et al. Expansion of the peri-implant attached gingiva with a three-dimensional collagen matrix in head and neck cancer patients-results from a prospective clinical and histological study. *Clin Oral Investig*. 2017;21:1103–1111.

4. Bottino MC, Thomas V, Schmidt G, et al. Recent advances in the development of GTR/GBR membranes for periodontal regeneration: a materials perspective. *Dent Mater*. 2012;28:703–721.

5. Al-Maawi S, Orlowska A, Sader R, James Kirkpatrick C, Ghanaati S. In vivo cellular reactions to different biomaterials—physiological and pathological aspects and their consequences. *Semin Immunol*. 2017;29:49–61.

6. Sheikh Z, Abdallah M-N, Hanafi AA, Misbahuddin S, Rashid H, Glogauer M. Mechanisms of in vivo degradation and resorption of calcium phosphate based biomaterials. *Mater (Basel, Switzerland)*. 2015;8:7913–7925.

7. Gottlow J. guided tissue regeneration using bioresorbable and non resorbable devices: initial healing and long term results. *J Periodontol*. 1993; 64(suppl):1157–1165.

8. Ghanaati S. Non-cross-linked porcine-based collagen I-III membranes do not require high vascularization rates for their integration within the implantation bed: a paradigm shift. *Acta Biomater*. 2012;8:3061–3072.

9. Ghanaati S, Barbeck M, Detsch R, et al. The chemical composition of

synthetic bone substitutes influences tissue reactions in vivo. *Biomed Mater*. 2012;7:015005.

10. Ghanaati S, Fuchs S, Webber MJ, et al. Rapid vascularization of starch-poly(caprolactone) in vivo by outgrowth endothelial cells in co-culture with primary osteoblasts. *J Tissue Eng Regen Med*. 2011;5:e136–e143.

11. Barbeck M, Serra T, Booms P, et al. Analysis of the in vitro degradation and the in vivo tissue response to bi-layered 3D-printed scaffolds combining PLA and biphasic PLA/bioglass components: guidance of the inflammatory response as basis for osteochondral regeneration. *Bioact Mater*. 2017;2:208–223.

12. Peng K-T, Hsieh M-Y, Lin CT, et al. Treatment of critically sized femoral defects with recombinant BMP-2 delivered by a modified mPEG-PLGA biodegradable thermosensitive hydrogel. *BMC Musculoskelet Disord*. 2016;17:286.

13. Laurito D, Cugnetto R, Lollobrigida M, et al. Socket preservation with d-PTFE membrane: histologic analysis of the newly formed matrix at membrane removal. *Int J Periodontics Restorative Dent*. 36:877–883.

14. Elgali I, Turri A, Xia W, et al. Guided bone regeneration using resorbable membrane and different bone substitutes: Early histological and molecular events. *Acta Biomater*. 2016;29:409–423.

15. Iosifidis MI, Tsarouhas A. Allografts in anterior cruciate ligament reconstruction. In: Doral M, Karlsson J, eds. *Sports Injuries*. Berlin: Springer; 2012:421–430.

16. Barbeck M, Udeabor S, Lorenz J, et al. High-temperature sintering of xenogeneic bone substitutes leads to increased multinucleated giant cell formation: in vivo and preliminary clinical results. *J Oral Implantol*. 2015;41: e212–e222.

17. Barbeck M, Udeabor SE, Lorenz J, et al. Induction of multinucleated giant cells in response to small sized bovine bone substitute (Bio-Oss) results in an enhanced early implantation bed vascularization. *Ann Maxillofac Surg*. 2014;4:150–157.

18. Barbeck M, Najman S, Stojanovic S, et al. Addition of blood to a phycogenic bone substitute leads to increased in vivo vascularization. *Biomed Mater*. 2015;10:55007.

19. Ghanaati S, Barbeck M, Booms P, Lorenz J, Kirkpatrick CJ, Sader RA. Potential lack of "standardized" processing techniques for production of allogeneic and xenogeneic bone blocks for application in humans. *Acta Biomater*. 2014;10:3557–3562.

20. Chia-Lai P-J, Orlowska A, Al-Maawi S, et al. Sugar-based collagen membrane cross-linking increases barrier capacity of membranes. *Clin Oral Investig*. 2018;22:1851–1863.

21. Schwarz F, Rothamel D, Herten M, Sager M, Becker J. Angiogenesis pattern of native and cross-linked collagen membranes: an immunohistochemical study in the rat. *Clin Oral Implants Res*. 2006;17:403–409.

22. Vepari C, Kaplan DL. Silk as a biomaterial. *Prog Polym Sci*. 2007;32: 991–1007.

23. Unger RE, Wolf M, Peters K, Motta A, Migliaresi C, Kirkpatrick JC. Growth of human cells on a non-woven silk fibroin net: a potential for use in tissue engineering. *Biomaterials*. 2004;25:1069–1075.

24. Brodbeck WG, Nakayama Y, Matsuda T, Colton E, Ziats NP, Anderson JM. Biomaterial surface chemistry dictates adherent monocyte/macrophage cytokine expression in vitro. *Cytokine*. 2002;18:311–319.

25. Anderson JM, Rodriguez A, Chang DT. Foreign body reaction to biomaterials. *Semin Immunol*. 2008;20:86–100.

26. Miron RJ, Bosshardt DD. Multinucleated giant cells: good guys or bad guys? *Tissue Eng Part B Rev*. 2018;24:53–65.

27. Barbeck M, Booms P, Unger R, et al. Multinucleated giant cells in the implant bed of bone substitutes are foreign body giant cells: new insights into the material-mediated healing process. *J Biomed Mater Res Part A*. 2017;105:1105–1111.

28. Zhang Y, Al-Maawi S, Wang X, Sader R, Kirkpatrick CJ, Ghanaati S. Biomaterial-induced multinucleated giant cells express proinflammatory signaling molecules: a histological study in humans. *J Biomed Mater Res Part A*. 2019;107:780–790.

29. Ghanaati S, Schlee M, Webber MJ, et al. Evaluation of the tissue reaction to a new bilayered collagen matrix in vivo and its translation to the clinic. *Biomed Mater*. 2011;6:15010–15012.

30. Barbeck M, Lorenz J, Kubesch A, et al. Porcine dermis-derived collagen membranes induce implantation bed vascularization via multinucleated giant cells: a physiological reaction? *J Oral Implantol*. 2015;41:e238–e251.

31. Barbeck M, Lorenz J, Holthaus MG, et al. Porcine dermis and pericardium-based, non-cross-linked materials induce multinucleated giant cells after their in vivo implantation: a physiological reaction? *J Oral Implantol*. 2015;41:e267–e281.

32. Omar O, Dahlin A, Gasser A, Dahlin C. Tissue dynamics and regenerative outcome in two resorbable non-cross-linked collagen membranes for guided bone regeneration: a preclinical molecular and histological study in vivo. *Clin Oral Implants Res*. 2018;29:7–19.

33. Al-Maawi S, Vorakulpipat C, Orlowska A, et al. In vivo implantation of a bovine-derived collagen membrane leads to changes in the physiological cellular pattern of wound healing by the induction of multinucleated giant cells: an adverse reaction? *Front Bioeng Biotechnol*. 2018;6:104.

34. Figueiredo M, Henriques J, Martins G, Guerra F, Judas F, Figueiredo H. Physicochemical characterization of biomaterials commonly used in dentistry as bone substitutes: comparison with human bone. *J Biomed Mater Res Part B Appl Biomater*. 2010;92B:409–419.

35. Benke D, Olah A, Möhler H. Protein-chemical analysis of Bio-Oss bone substitute and evidence on its carbonate content. *Biomaterials*. 2001; 22:1005–1012.

36. Ghanaati S, Barbeck M, Orth C, et al. Influence of β-tricalcium phosphate granule size and morphology on tissue reaction in vivo. *Acta Biomater*. 2010;6:4476–4487.

37. Barbeck M, Dard M, Kokkinopoulou M, et al. Small-sized granules of biphasic bone substitutes support fast implant bed vascularization. *Biomatter*. 2015;5:e1056943.

38. Ghanaati SM, Thimm BW, Unger RE, et al. Collagen-embedded hydroxylapatite-beta-tricalcium phosphate-silicon dioxide bone substitute granules assist rapid vascularization and promote cell growth. *Biomed Mater*. 2010;5:25004.

39. Ghanaati S, Orth C, Barbeck M, et al. Histological and histomorphometrical analysis of a silica matrix embedded nanocrystalline hydroxyapatite bone substitute using the subcutaneous implantation model in Wistar rats. *Biomed Mater*. 2010;5:035005.

40. Ghanaati S, Barbeck M, Hilbig U, et al. An injectable bone substitute composed of beta-tricalcium phosphate granules, methylcellulose and hyaluronic acid inhibits connective tissue influx into its implantation bed in vivo. *Acta Biomater*. 2011;7:4018–4028.

41. Fujioka-Kobayashi M, Schaller B, Saulacic N, Zhang Y, Miron RJ. Growth factor delivery of BMP9 using a novel natural bovine bone graft with integrated atelo-collagen type I: biosynthesis, characterization, and cell behavior. *J Biomed Mater Res Part A*. 2017;105:408–418.

42. Ghanaati S, Barbeck M, Detsch R, et al. The chemical composition of synthetic bone substitutes influences tissue reactions in vivo: histological and histomorphometrical analysis of the cellular inflammatory response to hydroxyapatite, beta-tricalcium phosphate and biphasic calcium phosphate ce. *Biomed Mater*. 2012;7:015005.

43. Gottlow J. Guided tissue regeneration using bioresorbable and non-resorbable devices: initial healing and long-term results. *J Periodontol*. 1993;64(11 suppl):1157–1165.

44. Lorenz J, Barbeck M, Kirkpatrick C, Sader R, Lerner H, Ghanaati S. Injectable bone substitute material on the basis of beta-TCP and hyaluronan achieves complete bone regeneration while undergoing nearly complete degradation. *Int J Oral Maxillofac Implants*. 2018;33:636–644.

45. Lorenz J, Barbeck M, Sader RA, et al. Foreign body giant cell-related encapsulation of a synthetic material three years after augmentation. *J Oral Implantol*. 2016;42:273–277.

46. Ghanaati S, Barbeck M, Willershausen I, et al. Nanocrystalline hydroxyapatite bone substitute leads to sufficient bone tissue formation already after 3 months: histological and histomorphometrical analysis 3 and 6 months following human sinus cavity augmentation. *Clin Implant Dent Relat Res*. 2013;15:883–892.

47. Lorenz J, Schlee M, Al-Maawi S, Chia P, Sader RA, Ghanaati S. Variant purification of an allogeneic bone block. *Acta Stomatol Croat*. 2017;51:141–147.

48. Dadsetan M, Jones JA, Hiltner A, Anderson JM. Surface chemistry mediates adhesive structure, cytoskeletal organization, and fusion of macrophages. *J Biomed Mater Res*. 2004;71A:439–448.

49. Brodbeck WG, Patel J, Voskerician G, et al. Biomaterial adherent macrophage apoptosis is increased by hydrophilic and anionic substrates in vivo. *Proc Natl Acad Sci U S A*. 2002;99:10287–10292.

50. McNally AK, Anderson JM. β1 and β2 integrins mediate adhesion during macrophage fusion and multinucleated foreign body giant cell formation. *Am J Pathol*. 2002;160:621–630.

51. McNally AK, Anderson JM. Phenotypic expression in human monocyte-derived interleukin-4-induced foreign body giant cells and

macrophages in vitro: dependence on material surface properties. *J Biomed Mater Res A*. 2015;103:1380–1390.

52. Lucke S, Walschus U, Hoene A, et al. The *in vivo* inflammatory and foreign body giant cell response against different poly(l-lactide-co-d/l-lactide) implants is primarily determined by material morphology rather than surface chemistry. *J Biomed Mater Res Part A*. 2018;106:2726–2734.

53. Ahmed GJ, Tatsukawa E, Morishita K, et al. Regulation and biological significance of formation of osteoclasts and foreign body giant cells in an extraskeletal implantation model. *Acta Histochem Cytochem*. 2016; 49:97–107.

54. Lorenz J, Al-Maawi S, Sader R, Ghanaati S. Individualized titanium mesh combined with platelet-rich fibrin and deproteinized bovine bone: a new approach for challenging augmentation. *J Oral Implantol*. 2018;44:345–351.

55. Lorenz J, Kubesch A, Korzinskas T, et al. TRAP-positive multinucleated giant cells are foreign body giant cells rather than osteoclasts: results from a split-mouth study in humans. *J Oral Implantol*. 2015;41:e257–e266.